Model weighting for ISMIP6-Greenland based on observations and similarity among models

Journal:	*Annals of Glaciology*
Manuscript ID	AOG-94-0485
Manuscript Type:	Article
Date Submitted by the Author:	22-Nov-2024
Complete List of Authors:	Luo, Xiao; University at Buffalo, Department of Geology Crooks Nowicki, Sophie; University at Buffalo, Department of Geology
Keywords:	Ice-sheet modelling, Ice velocity, Ice thickness measurements

Abstract:	The Ice Sheet Model Intercomparison Project for CMIP6 (ISMIP6) resulted in a large number of ice sheet simulations from multiple ice sheet models. To-date, there are no model weighting studies that analyze or quantify the model performance and possible duplication of the ISMIP6 ice sheet models and the resulting effect on projections of mass loss. In this study, we adopt a model weighting scheme for the ISMIP6-Greenland that accounts for both model performance compared to observation and model similarity due to possible duplication. We choose ice velocity and thickness for the measurement of model performance, and we use as many variables as we can to compute similarity indexes. For quality weight, we choose a quality parameter that leads to reduction of ensemble bias for both present-day and future projection. For similarity weight, we use an intermediate parameter that efficiently highlights model independence. The total model weights are simply constructed as the multiplication of the quality and similarity weights. Finally, the sea level rise contribution from ISMIP6-Greenland is updated with the weights, and we find that, although the multi-model mean is not considerably shifted, the model spreads are reduced by applying the model weights.

Model weighting for ISMIP6-Greenland based on observations and similarity among models

Xiao Luo[1], Sophie Nowicki[1,2]

Author Information

[1]Department of Geology, College of Arts and Sciences, University at Buffalo, State University of New York, Buffalo, NY, 14228, USA.

[2]RENEW Institute, College of Arts and Sciences, University at Buffalo, State University of New York, Buffalo, NY, 14228, USA.

Abstract

The Ice Sheet Model Intercomparison Project for CMIP6 (ISMIP6) resulted in a large number of ice sheet simulations from multiple ice sheet models. To-date, there are no model weighting studies that analyze or quantify the model performance and possible duplication of the ISMIP6 ice sheet models and the resulting effect on projections of mass loss. In this study, we adopt a model weighting scheme for the ISMIP6-Greenland that accounts for both model performance compared to observation and model similarity due to possible duplication. We choose ice velocity and thickness for the measurement of model performance, and we use as many variables as we can to compute similarity indexes. For quality weight, we choose a quality parameter that leads to reduction of ensemble bias for both present-day and future projection. For similarity weight, we use an intermediate parameter that efficiently highlights model independence. The total model weights are simply constructed as the multiplication of the quality and similarity weights. Finally, the sea level rise contribution from ISMIP6-Greenland is updated with the weights, and we find that, although the multi-model mean is not considerably shifted, the model spreads are reduced by applying the model weights.

1 Introduction

Greenland ice sheet mass loss has shown a large contribution to global sea level rise in the past decades (Shepherd and others, 2020) and will continue to play an important role in future sea level rise under a warming globe (Hofer and others, 2020; Fox-Kemper and others, 2021). The Ice Sheet Model Intercomparison Project for CMIP6 (ISMIP6) (Nowicki and others 2016, 2020) serves as an important estimator for ice sheet evolution in future, showing considerable spreads by the end of the 21st Century for the Greenland ice sheet (Goelzer and others, 2020; Payne and others, 2021). Following the approach taken by previous ice sheet community efforts such as Sea-level Response to Ice Sheet Evolution (SeaRISE; Nowicki and others 2013; Bindschadler and others 2013), the analysis of the ISMIP6 ice sheet model ensemble has adapted a "one model one vote" strategy.

The issues and drawback of assigning equal weights (also referred to as "one model one vote" strategy) have been extensively discussed in the climate modeling literature (Knutti, 2010; Knutti and others, 2010; Masson and Knutti, 2011; Pennell and Reichler, 2011; Knutti and others, 2017), but not detailly explored and discussed in the ice sheet modeling realm. There are existing studies that used calibration strategy, mostly via establishing Bayesian frameworks, to generate performance scores for either the Greenland or Antarctic ice sheet model ensemble (Gladstone and others, 2012; Ritz and others, 2015; DeConto and Pollard, 2016; Nias and others, 2019, 2023; Brinkerhoff and others, 2021; Aschwanden and Brinkerhoff, 2022; Felikson and others, 2023; Jager and others, 2024), but this approach is not yet applied on the ISMIP6 multi-model ensemble (for neither the Greenland nor Antarctic ice sheets). Furthermore, as these studies are mostly calibrating on single ice sheet model ensembles, the model inter-dependence is then not a pertinent topic because the ensemble members are essentially different realizations branching from the same model with varying controlling physics parameters.

Similar to the issues faced by climate models, the assignment of equal weights on ice sheet models have the following assumptions: i) each ice sheet model in the ensemble has equal performance of capturing the present-day ice sheet state (e.g., ice thickness, surface ice velocity and temperature, etc.) and projecting the ice sheet evolution into the future; ii) all models in the ensemble are independently developed without any duplications or exchanges of modeling ideas, codes and subcomponents. For the first assumption, ice sheet models obviously do not perform equally even at their initial states, which can be easily shown by the model errors of ice velocity and thickness compared to observation documented in SeaRISE (Nowicki and others 2013; Bindschadler and others 2013) and ISMIP6-Greenland (Goelzer and others, 2020). Also, it is highly unlikely that the models will all have equal performance of projecting the ice sheet into the future.

As for the model inter-dependence, it is risky to assume the models are completely independent from one another and allow equal votes for them. Because it is common that the ice sheet models have similar initialization process (e.g., data assimilation using the same velocity or thickness) and close physical laws. If these similar simulations are counted repetitively, the unweighted model ensemble will be biased toward the repeated projections. This is true for ISMIP6-Greenland as multiple submissions come from the same ice sheet model. For example, the Ice-sheet and Sea-level System Model (ISSM; Larour and others 2012) has been used by multiple modeling group, and in some cases, a group might have submitted a number of simulations. The three ISSM submissions from AWI have identical configurations except that they are run under different spatial resolutions (Appendix A1, Goelzer and others 2020), thus, they are expected to be quite similar. In contrast, the ISSM simulations from other groups (e.g., JPL_ISSMPALEO) might have larger differences resulting from different initialization techniques and modeling choices that eventually lead to distinct sea level rise projections. These submissions are all considered as independent models in Goelzer and others (2020) and Payne and others (2021), motivating our interests to account for not just model performance but also model inter-dependence to better interpret the information provided by ISMIP6.

For the model weighting strategy, it is challenging to define the correct metrics (or diagnostics) to measure the model performance because it is very difficult to have a proper definition (or even quantitative metrics) of the general skills of models (Knutti and others 2017). When the simulations are scored based upon different metrics, each model could outperform the other models on one metric but underperform on another variable. No decisive conclusions may be properly drawn in terms of which metric is the "best one" or "most appropriate one". The choices of diagnostics might have significant influences on the performance weighting as demonstrated by both climate model weighting (Lorenz and others, 2018) and a recent Bayesian calibration research on single ice sheet model (Felikson and others, 2023). The latter study assigned weights using ice velocity, dynamic thickness change and mass balance separately as diagnostics for calibration, and showed largely different posterior distribution. Also, for the same diagnostic such as ice surface velocity, a complexity may arise from the initialization step of ice sheet models that opted to use data assimilation to approach the present-day status of the Greenland ice sheet. If the same observation is chosen to measure the quality or performance for this specific diagnostic, results are likely going to favor the models who chose the same observation for the data assimilation, while the other models who chose a different dataset maybe down scored.

Yet, it is not trivial to assign weights based on some metrics as shown in the climate modeling community that has been attempting to extract credible and reliable information from the multi-model ensemble. The Climate model Weighting by Independence and Performance project (ClimWIP; Brunner and others 2019, Merrifield and others 2020), following the previous work of Sanderson and others (2015) and Knutti and others (2017), has assigned weights to CMIP6 models that leads to reduction of the model spreads. A recent ClimWIP study (Brunner and others, 2020) utilized an updated version of this model weighting strategy, and found a reduction of model spreads and generally lower global temperature rise under both weak and strong climate scenarios. This reduction is because several climate models with strong warming received low weights.

In this study, we utilize the ClimWIP model weighting framework to assign model weights to Greenland ice sheet models that participated in ISMIP6-Greenland, in order to investigate if the model weighting shift sea level projections and to what extents. We limit our focus on the same variables as used in Goelzer and others (2020), which are ice velocity and thickness, to assign performance weights to models. However, we use as many variables as we can to produce independence weights because this metric does not depend on observation. Then we update the multi-model ensemble projections with the various weights. This paper proceeds as follow: Section 2 will provide an overview of the model weighting strategy and data utilized for the weighting. Section 3 will describe the reasoning of choosing free parameters involved in the model weighting, the final results of model weights, and the updated model projections with weights. Section 4 will conclude this paper and provide discussion of limitations of this study and future research.

2 Data and Methods

2.1 Model weighting scheme

In this study, we adopt a model weighting scheme (Sanderson and others, 2015, 2017; Knutti and others, 2017) designed for model weighting of CMIP5 GCMs based on comparison of model simulation and observational data. This scheme is generally applicable for process-based model weighting, as it accounts for both the performance of model simulation and the similarity of a certain model in a multi-model ensemble due to possible duplication of codes and components.

In short, a certain model is weighted by both skill and independence. Essentially, the weight of a model w_i is determined via two parameters: (1) the weight of quality w_q, which measures how close the simulation approaches the observed values; (2) the weight of uniqueness w_u, which rewards the model if it demonstrates uniqueness compared with other models in the ensemble and punishes a certain model if it shows more replications. The total weight w_i is then evaluated as the multiplication of these two quantities as shown in Eq. (1):

$$w_i = w_q \times w_u = \exp[-(\frac{D_{i(obs)}}{D_q})^2] \times \frac{1}{1+\sum_{j\neq i}^{m}\exp[-(\frac{D_{ij}}{D_u})^2]} \tag{1}$$

where $D_{i(obs)}$ is the distance of the ith model from the true observation, and D_{ij} is the model similarity between a model pair. Following the method described in Sanderson and others (2017), we evaluate both $D_{i(obs)}$ and D_{ij} as Root Mean Square Errors (RMSEs). The pairwise distances are calculated for each variable and then linearly combined to formulate the distance matrices. For each variable, only the grid cells where all models and observation have valid values are retained to compute the distances, and other grids are removed. D_u and D_q are free parameters, representing the radius of uniqueness and radius of quality, respectively. They are quantified as percentiles of the mean of the inter-model distances, and we explore the choices of these two parameters in later sections.

Observations are necessary to quantify the weights of quality, but they are not needed to measure the weights of uniqueness (interchangeable with weights of similarity). Therefore, we use the variables described in Section 2.2 for quality weighting, and we use the simulated quantities mentioned in Section 2.3 to produce similarity weighting. Finally, all fields are normalized before they are used to compute the weights.

2.2 Simulation and observation data for quality weighting

The simulated ice thickness and ice velocity fields (Figures 1a and 2a) are used directly from the outputs of ISMIP6-Greenland (Goelzer and others, 2020). We use the snapshots of ice velocity and thickness at the beginning of the control projection ("ctrl_proj" hereafter) to compare with the observation datasets. We note that not all ice sheet models report surface ice velocity, for instance, the Greenland ice sheet models BGC_BISICLES, IMAU-IMAUICE1 and IMAU-IMAUICE2 only provide vertically averaged ice velocity fields, as these three models are run under either Shallow-Ice Approximation (SIA) or Shallow-Shelf Approximation (SSA). In order to maintain consistency with Goelzer and others (2020), which compares the vertically averaged velocity with observation, we use the same mean velocity to compare with observation. The ice thickness observation (Figure 1b) is obtained from BedMachine datasets (Morlighem and others, 2017, 2020). The observed surface ice velocity fields (Figure 2b) are obtained from MEaSUREs Greenland Ice Sheet Velocity Map from InSAR Data, Version 2 (Joughin and others, 2015) for Greenland ice sheet. The coverage of satellite mosaics varies from year to year, particularly in the southeast of the Greenland ice sheet. We use the 2016-2017 mosaics for Greenland that were produced mostly from Sentinel-1A/1B data and provided almost complete coverage over southeast region. The same period is used for ISMIP6-Greenland for model weighting regarding surface velocity.

For Figures 1 and 2, we use both heatmaps and Taylor diagrams (Taylor, 2001) to visualize the inter-model distances as well as model differences compared to observations. In a heatmap, each grid cell shows the value of distance between either a model pair, or model and observation (last row in Figure 1c). In a Taylor diagram, the RMSE, the standard deviation, and the Pearson correlation between models and observation are shown. Note that the values shown in both heatmaps and Taylor diagrams are normalized, and the red crosses in the Taylor diagrams (Figures 1d and 2d) correspond to the observations shown in Figures 1b and 2b. From the last row in Figure 1c, three models show close representation of ice thickness compared to observation (GSFC_ISSM, UAF_PISM1, and UAF_PISM2). In contrast, UCIJPL_PISM1 and VUW_PISM show largest differences with observation.

The relationships between model pairs are also captured in the heatmap (Figure 1c) as well. For instance, the three ISSM submissions from AWI show very small differences among each other, indicating that they are quite similar. This is expected because these three submissions start from the same initial ice sheet status and their major differences are mainly the minimum horizontal resolutions and mesh grids. From the Taylor diagram of ice thickness (Figure 1d), all models show high correlation (from 0.95 to 0.99) with observation, meaning that all models capture the spatial features of thickness very well. This can be anticipated from Figures 1a and 1b. In addition, the distances from models to observation are also shown as radial distances from models to the reference point in the Taylor diagrams. For example, VUW_PISM is quite far from the reference point, indicating that it is quite different from the thickness observation.

For ice velocity comparison, from the heatmap in Figure 2c, there are clearly some models who show large differences of ice velocity compared to observation (e.g., MUN_GISM1, LSCE_GRISLI, VUB_ GISM, and VUW_PISM). However, the heatmap scales by all distances and some pair-wise model distances are even larger than their differences to the observation, leading to less dissimilarity regarding which model deviates further from observation. On the other hand, the Taylor diagram has more focus on the model differences and correlation to the observation. For instance, both VUB_GISM and VUW_PISM show almost equally large differences compared to observation (Figure 2c), while the Taylor diagram (Figure 2d) demonstrates that VUB_GISM is more different than VUW_PISM from the observation. We notice that all ISSM submissions match the observation quite well except JPL_ISSMPALEO. This is because it used longer period of interglacial spin-up while others used data assimilation of the ice velocity that matches better with present-day observation, such as AWI_ISSMs and GSFC_ISSM. Note that the ISSM submissions from JPL used different velocity datasets (Rignot and Mouginot, 2012, 2008–2009) for data assimilation; therefore, this might add to the distance from model to observation because we use velocity data from Joughin and others (2015) as observation.

In summary, models often demonstrate different performance compared to different observations. For example, JPL_ISSMPALEO and MUN_GSM2 show large differences to observed thickness but smaller differences to observed velocity, while some models (e.g., VUB_GISM and VUW_PISM) show the opposite. This highlights the value of using both variables for quality weighting for the remaining of this study.

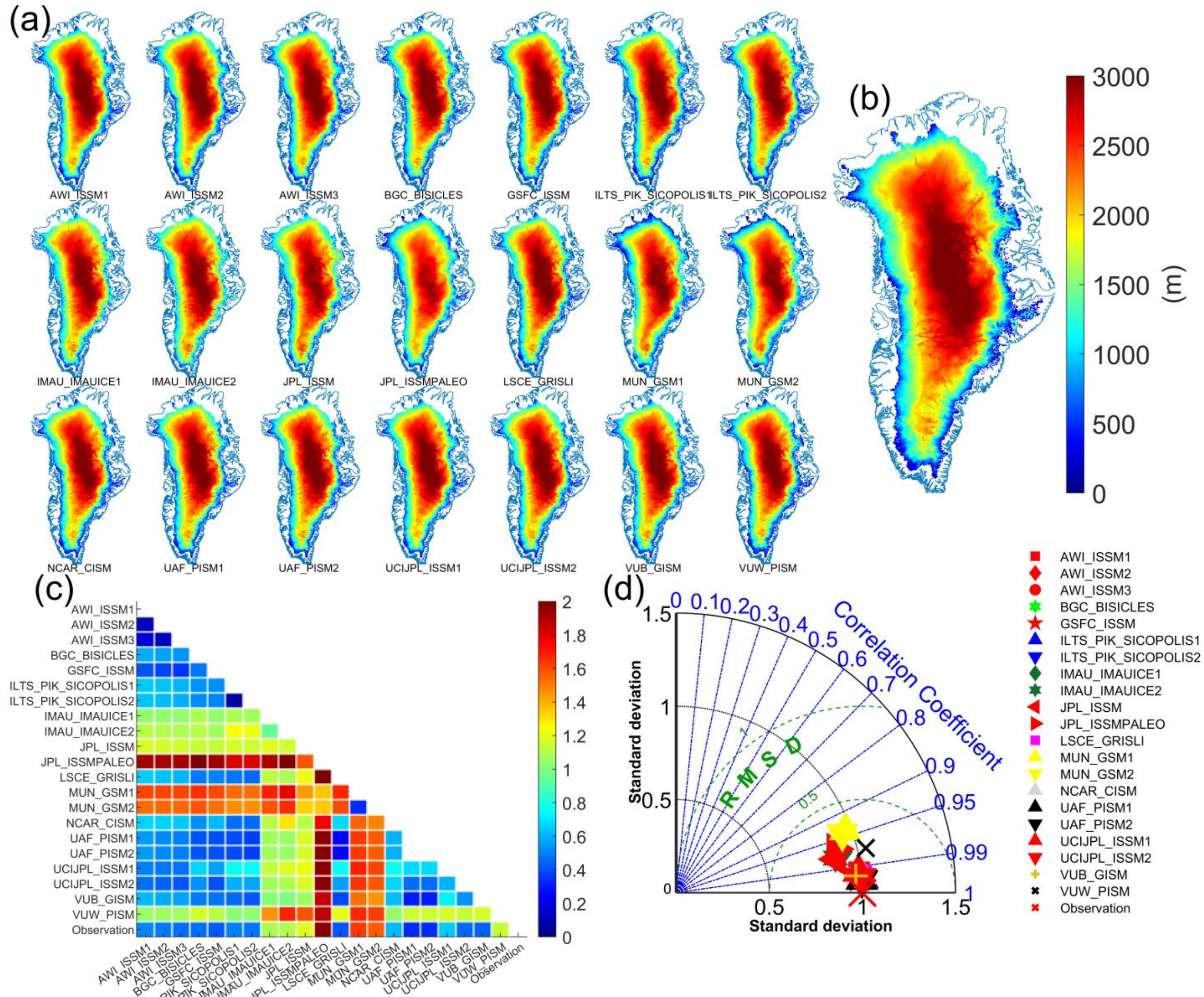

Fig. 1. Greenland ice thickness field in 2015 of (a) ISMIP6-Greenland ice sheet models and (b) observed ice thickness obtained from BedMachine datasets (Morlighem and others, 2017, 2020). The differences between model pairs and model-observation are visualized with (c) heatmap and (d) Taylor diagram. Note that the values shown in (c) and (d) are normalized, and the red cross in (d) corresponds to the observation shown in (b).

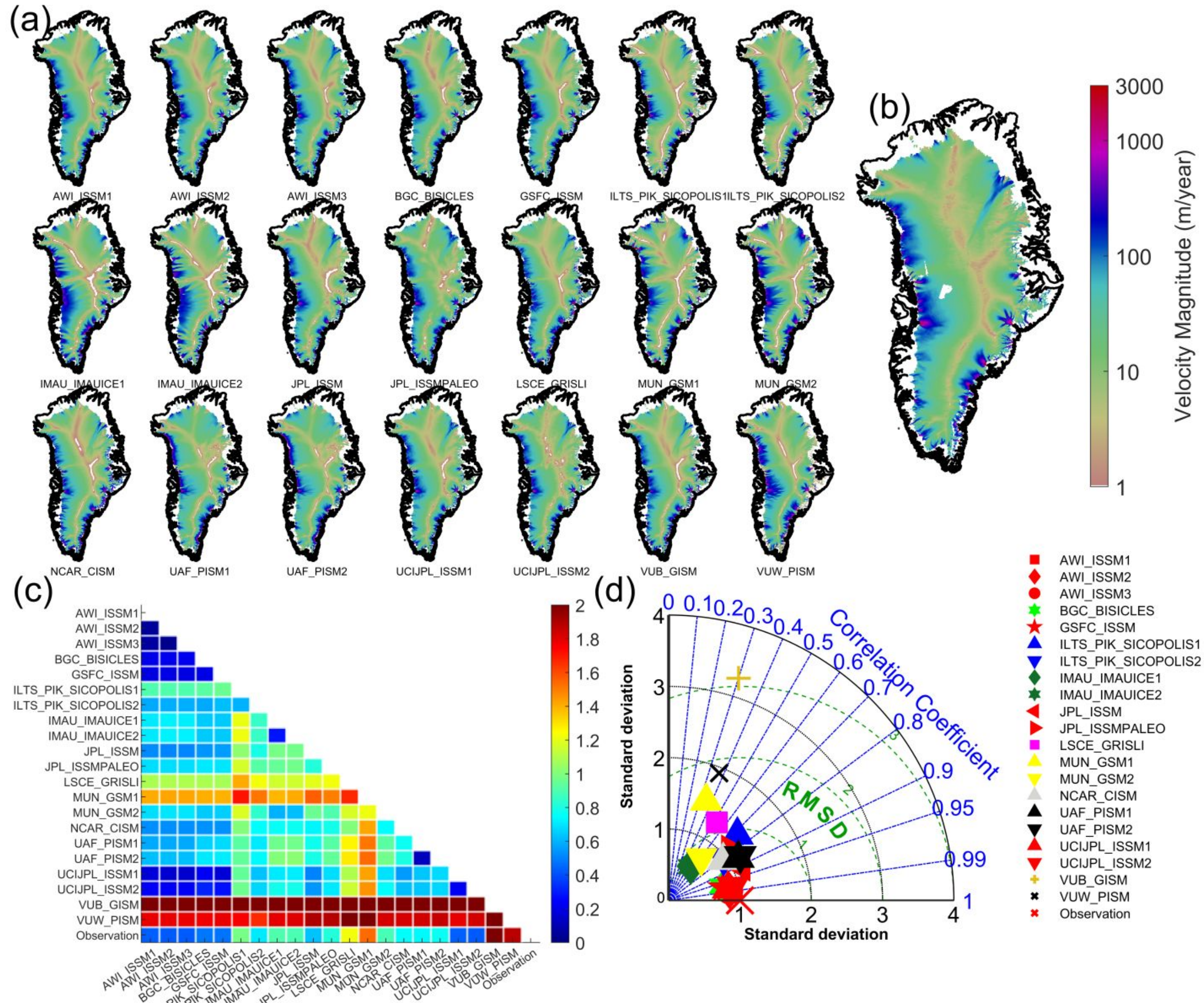

Fig. 2. Greenland vertically averaged ice velocity field in 2017 of (a) ISMIP6-Greenland ice sheet models and (b) observed ice velocity obtained from MEaSUREs Greenland Ice Sheet Velocity Map from InSAR Data, Version 2 (Joughin and others, 2015). The differences between model pairs and model-observation are visualized with (c) heatmap and (d) Taylor diagram. Note that the values shown in (c) and (d) are normalized, and the red cross in (d) corresponds to the observation shown in (b).

2.3 ISMIP6 data for similarity weighting

Since the similarity weighting does not require a complete set of corresponding observational data for each field considered, we use as many fields as we can to calculate the model similarity weights, except for those variables with more than five models that do not have simulations in the first year of “ctrl_proj”. This gives a reasonable size of variables that we can use for similarity weighting. The fields used to produce similarity weight are tabulated in Table 1. The other variables in the data repository are not considered because there are more than 5 models who do not report them.

Table 1. ISMIP6 variables used to generate similarity weighting.

	Variable Name	Variable	Units
1	acabf	Surface mass balance flux	kg m-2 s-1
2	dlithkdt	Ice thickness imbalance	m s-1
3	hfgeoubed	Geothermal heat flux	W m-2
4	litempbotgr	Basal temperature beneath grounded ice sheet	kg m-2 s-1
5	litemptop	Surface temperature	K
6	lithk	Ice thickness	m
7	orog	Surface elevation	m
8	topg	Bedrock elevation	m
9	xvelbase	Basal velocity in x-direction	m s-1
10	xvelmean	Mean velocity in x-direction	m s-1
11	yvelbase	Basal velocity in y-direction	m s-1
12	yvelmean	Mean velocity in y-direction	m s-1

We take each variable tabulated in Table 1 directly from the ISMIP6-Greenland dataset and reshape the field into a vector. The distances between each pair of models are evaluated as RMSE. The inter-model distances are then shown as heatmaps utilizing data from different times: initial state (Figure 3a), 2100 in exp05 (Figure 3b), 2100 in all experiments excluding control and control projection (Figure 3c), and averaged values of initial state and 2100 in all experiments (Figure 3d). The reason why we want to test model similarity beyond the initial state of ice sheet is that, despite its large influence on the future ice sheet evolution as shown in Goelzer and others (2018), similar initial condition does not always guarantee that a pair of models are truly similar, even if they are from the same modeling group. Although they maybe initialized in an identical fashion, they can respond differently to climate forcing due to different modeling choices in the projections, eventually leading to distinct sea level rise. Therefore, we use both the initial condition of ice sheet in the beginning year of "ctrl_proj" experiment and the future response in the last year of different experiments to measure the proximity of models.

For model distances shown in Figure 3b, we use exp05 for all models except for UAF_PISM2 that uses expc01 because it is the only model that did not participate in exp05. For the heatmap in Figure 3c, all experiments are considered to generate the model distances, and we do not need to make substitutions for UAF_PISM. In the case when not all models participated in an experiment, then the distances are only computed using the available models. Finally, the model distances are averaged over each experiment. Figure 3d shows the average values of Figures 3a and 3c.

We observe that the three submissions from AWI_ISSM have the smallest model distances to other models in the ensemble, which can be seen from both initial state (Figure 3a) and future projections (Figures 3b and 3c). JPL_ISSM, JPL_ISSMPALEO, MUN_GISM1 and GISM2, UAF_PISM1 and PISM2, and VUW_PISM show largest model differences with other models for both initial state (Figure 3a) and future projections in exp05 (Figure 3b), while VUW_PISM is less distinct when all experiments are considered (Figure 3c). We also note that the model distances are smaller when using future projections in exp05 (Figure 3b) compared to using initial state only (Figure 3a). This motivates the utilization of both initial state and future projection for the similarity measurement. However, the usage of only one experiment may not fully capture model behaviors because ice sheet models may respond similarly to one set of climate forcing but differently to another. For instance, one ice sheet model may be sensitive to high atmospheric forcing but not oceanic forcing, and ISMIP6 project was designed to sample their different responses to climate forcing (Table 3 in Nowicki et al 2020). In addition, ice sheet models may have different ocean forcing strategies (standard or open experiments) such as UAF_PISM1 and UAF_PISM2. Therefore, it is meaningful to explore the complete set of experiments for model similarity.

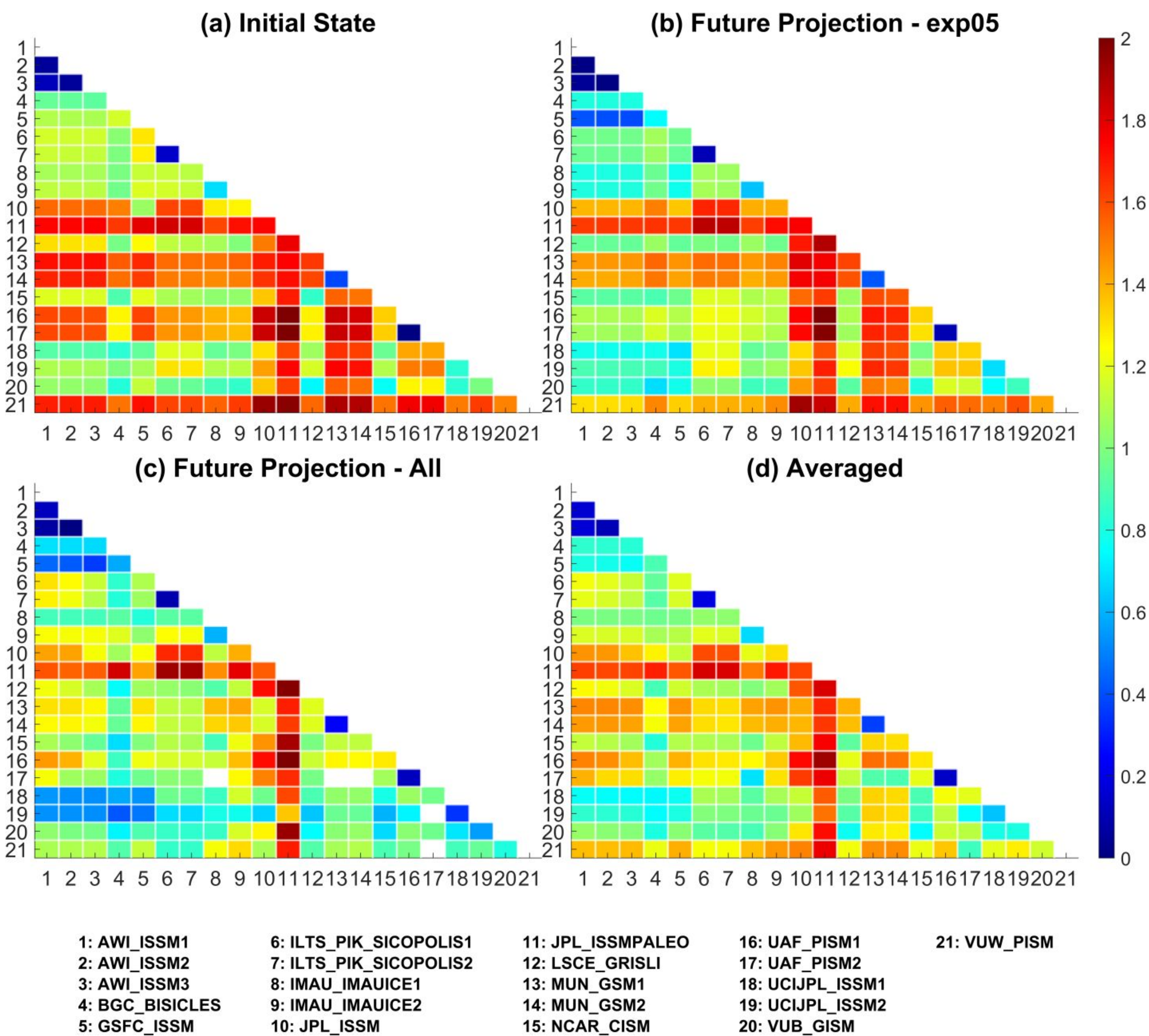

Fig. 3. A heatmap representation of the inter-model distances of ISMIP6-Greenland models using the variables list in Table 1 from (a) initial condition, (b) 2100 in exp 05 (with UAF_PISM1 using expc01), (c) 2100 in all experiments. The averaged inter-model distance of (a) and (c) is shown in (d).

3 Results

3.1 Similarity weighting

As mentioned in Data and Method, the radius of uniqueness D_u representing the nearest distance of one model is a free parameter; therefore, we show the similarity weights of each model with varying uniqueness radii expressed as percentiles of the mean of the intermodal distances in Figure 4. The similarity weights are separately computed using initial condition (Figure 4a), 2100 in exp05 (Figure 4b), and 2100 in all experiments (Figure 4c). The averaged values from Figures 4a and 4c are shown in Figure 4d.

From the approach in Knutti and others (2017), it is ideal to select a D_u that produces nearly $1/N$ of similarity weights for the same model with different variants (N is the number of variants submitted to ISMIP6). For example, as there are 8 submissions of ISSM, then each of them receiving 1/8 of weight is an ideal case; whereas SICOPOLIS receiving a weight of 0.5 is ideal as it has two submissions. However, there does not seem to be an optimal value of D_u that yields approximately $1/N$ of similarity weights for all models (Figure 4). In addition, this philosophy taken in the climate model community might not apply here as there are many different physics options and initialization methods for the same ice sheet model that could lead to very different model simulations. For example, ISSM carried out by AWI is quite distinct from the simulations by JPL. Indeed, from all panels in Figure 4, the three ISSM simulations of AWI receive low weights of similarity due to their similar simulations among themselves and also with other models, while the two ISSM submissions from JPL are distinct from all other models resulting in higher similarity weights.

In this study, we pick an intermediate value of 50% of the mean of inter-model distance as the similarity radius D_u (Figure 4). With D_u smaller than this value, most models are given similar weights and there is essentially little weighting effect. With radius approaching larger values, most weights are put on a few models that are most unique, which also results in little weighting effect on all other models because the rest of them are almost equally downweighed. The two variants of UAF_PISM have almost identical initial conditions, so they would have received much lower weights using “ctrl_proj” only (Figure 4a); however, UAF_PISM1 show considerably different response (compared to all other models including UAF_PISM2), which leads to higher weights (Figure 4c). This highlights the value of using both initial condition and future response to measure model behavior and their similarities (Figure 4d). We also notice the difference between UAF_PISM1 and UAF_PISM2 are not demonstrated using exp05 only (Figure 4b) because they respond very similarity to the climate. Eventually, we use the 50% of mean inter-model distance as D_u shown in Figure 4d.

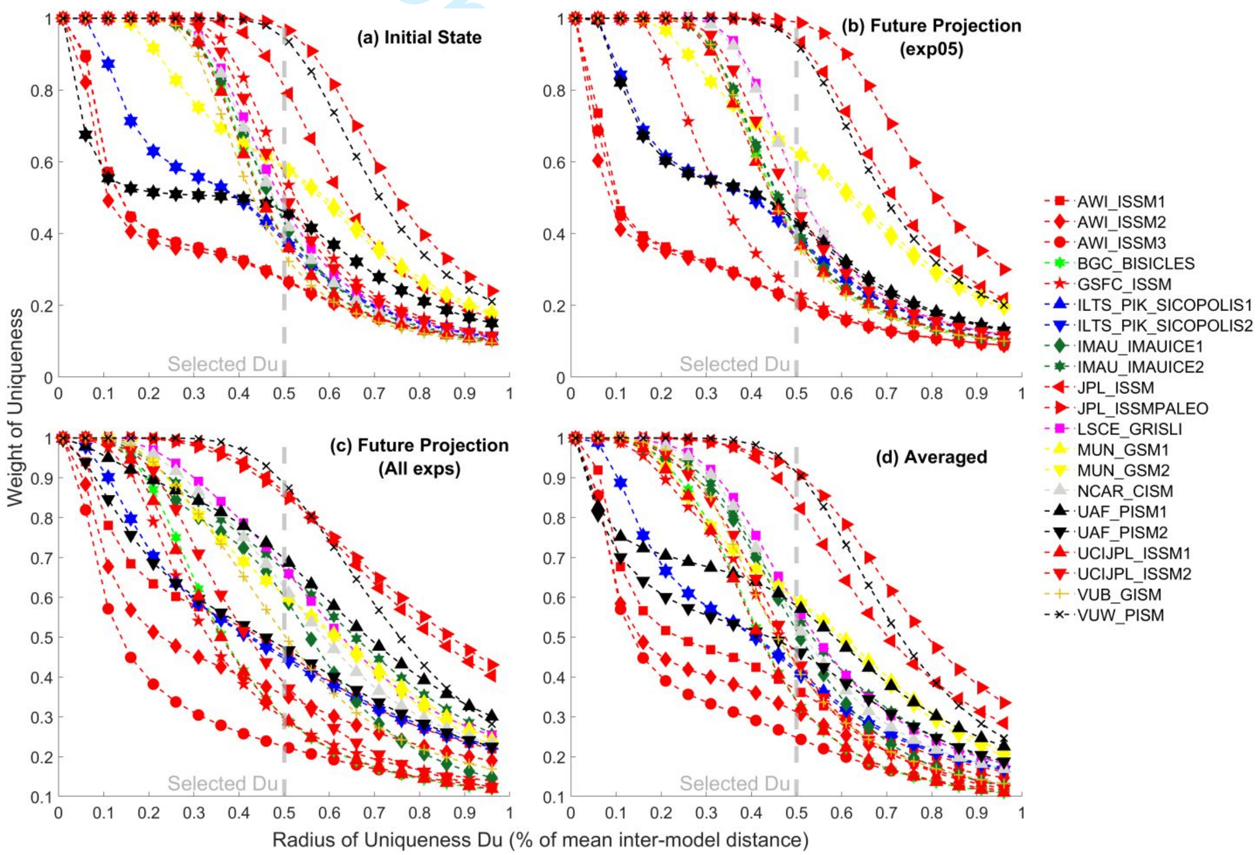

Fig. 4. Weight of similarity of ISMIP6-Greenland models with varying radius of uniqueness D_u measured as percentiles of mean inter-model distances using (a) initial state, (b) 2100 in exp05 experiments and (c) 2100 in all experiments. The average weight of similarity is shown in (d), which is used as the final similarity weight under selected $D_u = 0.5$ times the mean of inter-model distance.

We perform the same practice as in Brunner and others (2020) to examine the validity of similarity weighting via a hierarchical clustering approach using the initial state, and the results are shown in Figure 5. The hierarchical clustering automatically sorts the similar models into the same family and formulates a complete family tree. When the distances (or cut-off) are large (beginning from the leftmost side), all models are sorted into the same family. The models are gradually sorted out to different branches in the tree when the cut-off is decreased until each model is its own family (the rightmost side of the family tree). Unsurprisingly, JPL_ISSMPALEO is the first one to formulate an independent branch. Other unique models that show considerably different initial conditions (See Section 2 Data and Methods) including VUW_PISM, MUN_GSM1 and MUN_GISM2 are also rapidly sorted out. The vertical line shows the same distance as in Figure 4. We can observe that, under this cut-off, the unique models (such as JPL_ISSMPALEO) are clearly distinguished from the others and the similar models are grouped into the same model family. For instance, the three ISSM simulations with AWI are grouped together, and the same applies to UAF_PISM (1 and 2), ILTS_PIK_SICOPOLIS (1 and 2), and IMAU_IMAUICE (1 and 2). GSFC_ISSM and JPL_ISSM are sorted into the same family but not with the other ISSMs from JPL and UCIJPL, indicating that our choice of similarity radius can still highlight the differences among these ISSM models.

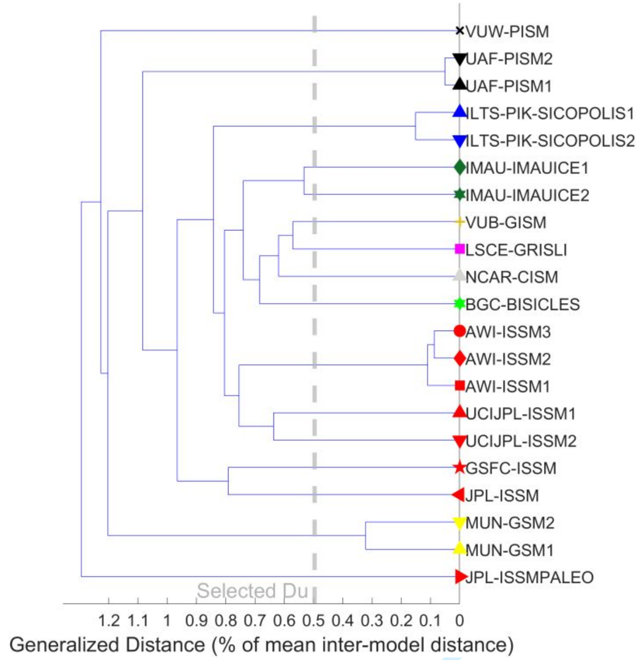

Fig. 5. Hierarchical clustering of ISMIP6-Greenland models using the initial conditions of control projections in 2015. The vertical line indicates the selected similarity radius, which is $D_u = 0.5$ times the mean of inter-model distance.

3.2 Quality weighting

The choice of the radius of quality D_q is also a free parameter, and we use similar tests as shown in Knutti and others (2017). Ideally, the chosen radius of quality should result in a decrease of RMSE of weighted results compared to the unweighted results. Therefore, we show the fraction of RMSE of weighted results compared to unweighted with varying quality radii measured as percentiles of the mean of model-observation distances (Figure 6). For both the velocity and the multivariate cases, strong quality weighting with narrow radius results in the largest decrease of RMSE, that is, when the skill radius equals around 20% of the mean of model-observation distances. However, the decrease of the present-day model difference from observation does not guarantee the weighted ensemble will have better performance in predicting the future. Thus, we also perform an out-of-sample test, and we show the results in Figure 6b. This test adds more confidence in choosing an appropriate quality radius that can likely improve the ensemble performance in future projection. The velocity and ice thickness of the "exp05" projection in the end of the 21st Century are used to conduct the out-of-sample test. Given that we obviously do not have the observation in 2100, the out-of-sample test iteratively treats each model projection in 2100 as the truth. The distances from the remaining models to this "truth" are computed, which are also measured as RMSEs, and then summed up. This iteration is applied to all models, and the obvious family members of each model are removed when it is treated as the "truth" model. For a certain model, if the distance to another model is smaller than its distance to observation, then this model is considered as its family member. The family models are indicated as black cells in Figure 6c. The diagonal is all removed since the model itself is obviously its family model. The fractions of RMSE of weighted ensemble to the unweighted (Figure 6b) suggest that extreme quality weighting with small quality radius does not necessarily reduce the bias in the future projection. Assigning excessive weights to only a few models (i.e., using a small quality radius), which have close agreement with the present-day observation, does not guarantee reduction of future projection bias, especially for ice thickness change (blue dotted curve in Figure 6b). Note that Figure 6a is constructed using the initial state in 2015 only, while 5b is using the last year in the "exp05" projection, which is 2100. Eventually, we choose the quality radius D_q as equal to the mean model-observation distance. This choice reduces both the present-day ensemble distance to observation and ensemble bias of future projection.

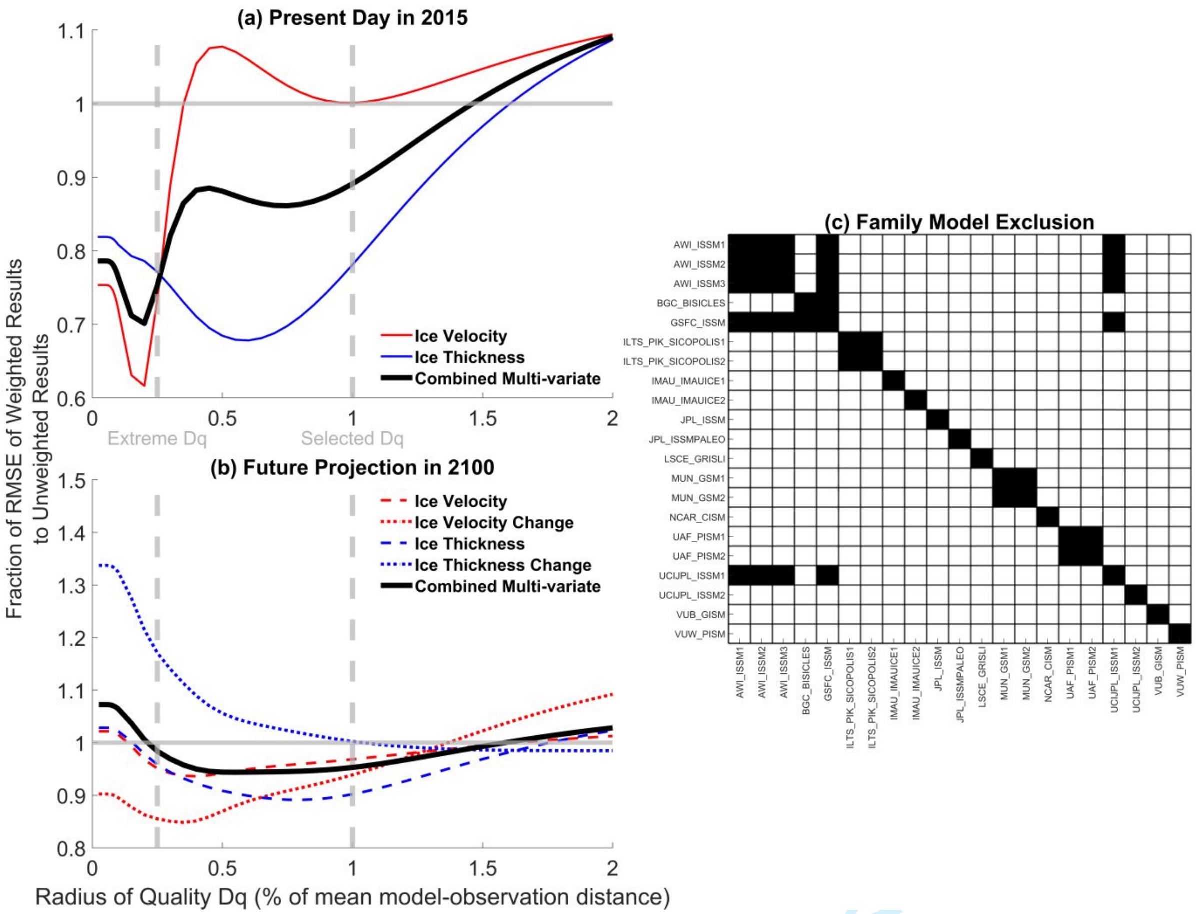

Fig. 6. The fraction of RMSE of weighted to unweighted results with varying radius of quality D_q measured as percentiles of mean model-observation distances using (a) the data in 2015 and (b) "exp05" experiment in 2100. The magnitude of ice velocity and thickness (dashed curves) and their changes from 2015 to 2100 (dotted curves) as well as the mean of above (solid curve) are shown in b. (c) The models that are excluded from the out-of-sample test when each model is treated as the truth. The black cells in (c) represent the excluded family models for each model. Finally, note that (a) is constructed using the initial state in 2015 of "ctrl_proj" only, while (b) is using the last year in the "exp05" projection, which is 2100.

3.3 Model weighting results

We show the final weighting results (Figure 7) in the same fashion as Sanderson and others (2015) with the x-axis showing the weights of similarity and y-axis the weights of quality. Total weights are indicated by the shaded areas, for example, if a model falls into the lower-left shaded area, then its total weight is between 0-0.1. We show the weighting results under both univariate quality weighting (Figure 7a using velocity only and 7b using ice thickness only) and combined weights (Figure 7c).

Obvious clustering behavior is observed for most models, for instance, most ISSM variants receive similar model weights, except the submissions from JPL, indicating the JPL submissions are quite different than rest of ISSMs. The ISSM submissions from AWI, GSFC, and UCIJPL and BGC_BISICLES used data assimilation for initialization that results in close agreement with present-day ice sheet state, and therefore these models receive higher quality weights for both velocity and thickness. However, since these models that opted for data assimilation have similar initial conditions, they receive lower similarity weights (x-axes in Figure 7). SICOPOLIS, IMAUICE, and GSM models, each having two submissions, also show little differences of model weights (for each pair), indicating each pair of submissions is quite similar. The PISM model simulated with VUW group is clearly distinguishable from the two PISM submissions from UAF group.

The same model may also receive different weights when either velocity or ice thickness is used to measure their performance. For instance, PISM submissions from UAF receive high weights for thickness but low weights for velocity. These two models use long inter-glacial spin-up and kept the ice surface close to observation using a flux correction method (Aschwanden and others, 2016), leading to their close representation of thickness but not for velocity. This highlights the need to use both velocity and thickness to measure the model performance instead of univariate as some models do not have equal performance regarding variables. In contrast, VUW_PISM receive low weights for both velocity and thickness due to that it used a different initialization method than submissions from UAF. VUW_PISM did not use flux correction, leading to its lower thickness weights. We notice that JPL_ISSM, JPL_ISSMPALEO, MUN_GSM1, and MUN_GSM2 receive very low weights for quality weighting using ice thickness. However, this does not mean they differ drastically from the observed thickness field over Greenland ice sheet (Figure 2), but they are comparatively less close to the observation than other models. This is by design of Sanderson's method (Equation 1). These models used long interglacial spin-up that leads to less constrained ice geometry, and MUN_GSM1 and MUN_GSM2 used different bedrock (Bamber and others, 2001) compared to the other models that used BedMachine (Morlighem and others 2017). Finally, we note that the models simulated by different groups may or may not be similar to each other, indicating it is worthwhile to treat each submission as an independent model.

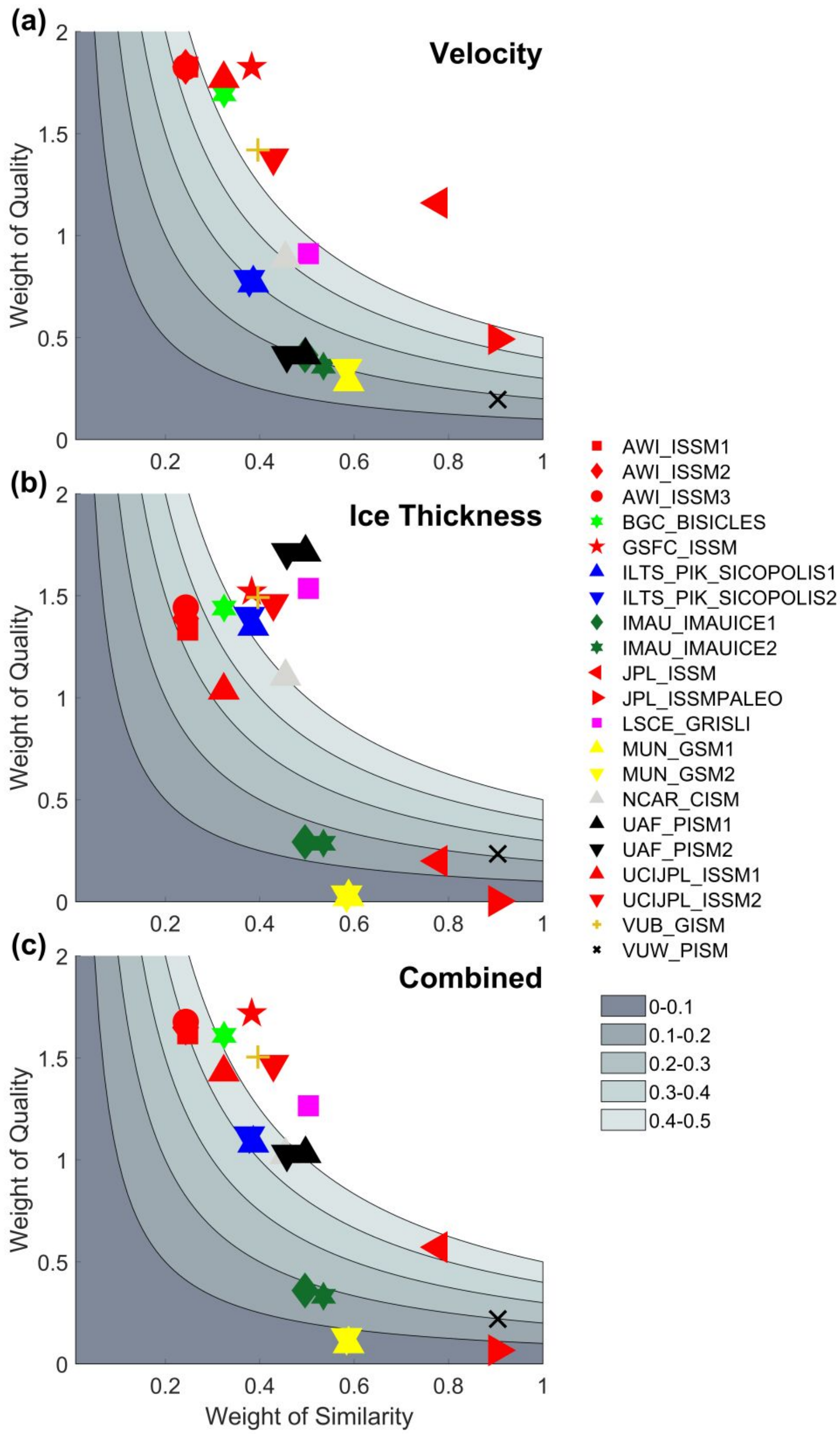

Fig. 7. Results of ISMIP6-Greenland model weights of similarity (x-axis), weights of quality (y-axis), and total weights (indicated with shaded area) where the quality weights are using (a) ice velocity only, (b) ice thickness only, and (c) both ice velocity and thickness. The legends show the markers for each model. The same color is used for the same model variants; for example, red color for all ISSMs.

3.4 Weighted ice sheet projections

The weights shown above in Section 3.3 are then used to produce the weighted sea level projections by ISMIP6-Greenland models (Table 2 and Figures 8-11). We pick the experiments shown in Figure 12 of Goelzer and others (2020) to demonstrate the weighting effects on the final sea level rise projections. In Table 2, we define the weighted ensemble mean as $\mu_{SLR} = \sum w_i \times SLR_i / \sum w_i$, and the weighted ensemble standard deviation (std) is defined as $\sigma_{SLR} = \sqrt{\sum_{i=1}^{N} w_i \times (SLR_i - \mu_{SLR})^2 / \sum_{i=1}^{N} w_i}$. For exploration purpose, we show the results with varying choices of weights in Table 2 including the total combined weights $w_i = w_q \times w_u$, quality weights only w_q, similarity weights only w_u, velocity weights only $w_i = w_{q(vel)} \times w_u$, and thickness weights only $w_i = w_{q(thickness)} \times w_u$.

We find that the multi-ensemble mean of sea level rise projections do not deviate much from the equal weighting case (mostly within $\pm 1\text{cm}$), indicating that the weighting has minimal effects on the ensemble mean. However, we notice that the model weights decrease the standard deviations (the “std reduction” rows in Table 2), and this decreasing effect varies among different experiments, ranging from minor effects (around -1%) to moderate decrease (around -30%). Using similarity weights only, the standard deviations are mostly increased, which can be anticipated because the similarity weighting is supposed to highlight the unique models, whose sea level projections may deviate more from the majority of the ensemble than others. For all other types of weights, the weighting effects have similar influences on the standard deviation decrease.

We also note that the weighted ensemble standard deviation is a simple statistical metric that does not take the data distribution of original ice sheet projections into account. Therefore, it does not directly translate to data spread. In order to explore how much the weights modify model spreads and shift data distribution, we use four different ways of applying the model weights on original ISMIP6-Greenland projections: direct approach (Figure 8), Monte Carlo sampling (Figure 9), bootstrap resampling (Figure 10), and kernel density estimation using Gaussian kernel (Figure 11). For the direct approach, the sea level projections are multiplied by the model weights in a straightforward manner, i.e., $SLE_{weighted} = SLE_{original} \times w_i$, where each model weight w_i is scaled up such that $\sum w_i$ equals to the number of models ($N = 21$). For the Monte Carlo sampling, we collect 2000 random samples with each sample randonly drawn from the original sea level rise projection, and set the probability of each model equal to its weight. The statistics of both the direct approach and the Monte Carlo approach are then summarized by the boxplots in Figures 8 and 9. Boostrap resampling collects 2000 samples as well, but each of them are randomly drawn with replacement that equal to the size of original samples ($N = 21$), in contrast to the Monte Carlo approach that draws only one value in each sample. We estimate the mean of sea level rise projections from the boostrap samples and plot the probability density functions (PDFs) in Figure 10. Finally, Kernel Density Estimation (KDE) builds directly upon original projections calibrated with the model weights, because it adjusts the peaks and standard deviations of the Gaussian kernels locally around each “data point” (in this case, each ISMIP6 projection). For instance, if a model has larger weight, then larger confidence is implied for this value; therefore, the Gaussian kernel of this point becomes taller and slimmer. We show the PDFs of KDE results in Figure 11, and the original ISMIP6 projections are marked on the x-axes as well.

In Figures 8 and 9, we simply define the model spread as the interquartile range (i.e., the middle 50-percentiles), which is the length of the box. The outliers are the models who deviate more than 1.5 times of the interquartile range from the ensemble mean, and these are marked as red crosses. The changes of model spreads are shown by the text near each box, measured as percentage of original model spread. Note that the y-axes have different scales so that they align to the total range of their original ISMIP6 simulations in Figure 9. For the direct approach, although the multi-model means have minor shifts, it gives much larger model spreads after applying the model weights as the original sea level rise projections are scaled either up or down by multiplying the weights. This increase is around 2 times larger for all weighting types except for the similarity weighting only. In contrast, the Monte Carlo approach gives mostly a reduction of the model spread. We observe that, by using total weights, most experiments have a decrease of model spread, with the magnitude of reduction ranging from zero (e.g., CSIRO-Mk3.6 Medium RCP8.5) to moderate (-19.19% for MIROC5 Low RCP8.5) values. The quality weights mostly have similar effects as the total weights. Under similar weighting only, the model spreads are moderately increased for some experiments, which can also be observed in Table 2 due to the same reasoning above. We also explore the impacts of univariate weighting as well. We find that the velocity weighting reduces model spreads for all experiments, while the effects of ice thickness on weighted ensemble are rather diverse among experiments. Ice thickness weighting alone does not always reduce the model spreads for all experiments, and a significant increase of spread (39.58%) is observed for CSIRO-Mk3.6

Medium RCP8.5 experiment. This increase is because three models which received high weights (BGC_BICICLES, LSCE_GRISLI2, and UAF_PISM2) each generated lower end sea level rise projections. This indicates the choice of using ice velocity alone to assign model weights based on present-day observation might be more optimal compared to univariate thickness weighting. Bootstrap resampling is used to estimate the distribution of sample mean and the results are shown in Figure 10. Note that this is not the distribution of sea level rise projections, but the estimation of the multi-model means. All weighting types except the similarity weighting scheme can reduce the variance of the distribution, which is similar to the results presented in Figure 9. Finally, we use kernel density estimation to construct the distribution of sea level projections with weights (Figure 11). The black thick curve shows the distribution of sea level rise projections, and all other curves show distributions with model weights. We observe that the distribution spreads are reduced for all Tier-1 core experiments including exp05, exp06, exp08 (the three exps in first row), exp09, exp10, and exp07 (the three exps in last row). In contrast, the Tier-2 experiments are less influenced by the choices of model weights.

In general, we conclude that the application of our model weights reduces the model spreads from minor to moderate levels depending on experiments, although it does not have major impacts on multi-model mean. Finally, we note that the model spreads shown in Figures 8-11 are not directly comparable to the standard deviations in Table 2 as they are different metrics.

Table 2. Weighted multi-model ensemble statistics of the chosen ISMIP6 experiments using various types of model weights.

Weight		Experiments								
Type	Statistics	exp05 MIROC5 Med RCP8.5	exp06 NorESM-M Med RCP8.5	exp08 HadGEM 2-ES Med RCP8.5	expa01 IPSL-CM5A-MR Med RCP8.5	expa02 CSIRO-Mk3.6 Med RCP8.5	expa03 ACCESS 1-3 Med RCP8.5	exp09 MIROC5 High RCP8.5	exp10 MIROC5 Low RCP8.5	exp07 MIROC5 High RCP2.6
Equal Weight	Mean (cm)	10.143	6.921	8.283	7.704	4.429	5.593	9.961	8.353	3.174
	Std (cm)	1.934	1.84	1.782	5.026	3.052	3.727	4.617	3.706	0.829
	Std Change	0	0	0	0	0	0	0	0	0
Total Weight	Mean (cm)	10.274	7.065	8.304	9.43	5.412	6.822	10.072	8.354	3.282
	Std (cm)	1.58	1.56	1.447	3.506	2.318	2.69	4.526	3.667	0.64
	Std Change	-18.30%	-15.22%	-18.81%	-30.26%	-24.04%	-27.81%	-1.98%	-1.05%	-22.80%
Quality Only	Mean (cm)	10.393	7.169	8.394	9.457	5.465	6.867	10.379	8.587	3.338
	Std (cm)	1.555	1.533	1.456	3.591	2.376	2.746	4.347	3.502	0.62
	Std Change	-19.58%	-16.66%	-18.26%	-28.56%	-22.15%	-26.32%	-5.84%	-5.52%	-25.26%
Similarity Only	Mean (cm)	9.824	6.659	8.016	7.377	4.225	5.341	9.199	7.751	3.015
	Std (cm)	1.955	1.841	1.741	5.068	3.056	3.747	4.946	4.027	0.905
	Std Change	1.09%	0.04%	-2.30%	0.82%	0.14%	0.54%	7.12%	8.65%	9.19%
Velocity Only	Mean (cm)	10.263	7.049	8.282	9.045	5.251	6.568	10.414	8.73	3.237
	Std (cm)	1.642	1.607	1.5	4.047	2.562	3.042	3.987	3.217	0.732
	Std Change	-15.09%	-12.66%	-15.80%	-19.49%	-16.04%	-18.37%	-13.65%	-13.19%	-11.75%
Thickness Only	Mean (cm)	10.183	6.978	8.231	9.496	5.395	6.849	9.647	7.952	3.27
	Std (cm)	1.582	1.583	1.456	3.264	2.223	2.543	4.905	3.968	0.621
	Std Change	-18.20%	-13.95%	-18.28%	-35.06%	-27.16%	-31.76%	6.24%	7.06%	-25.13%

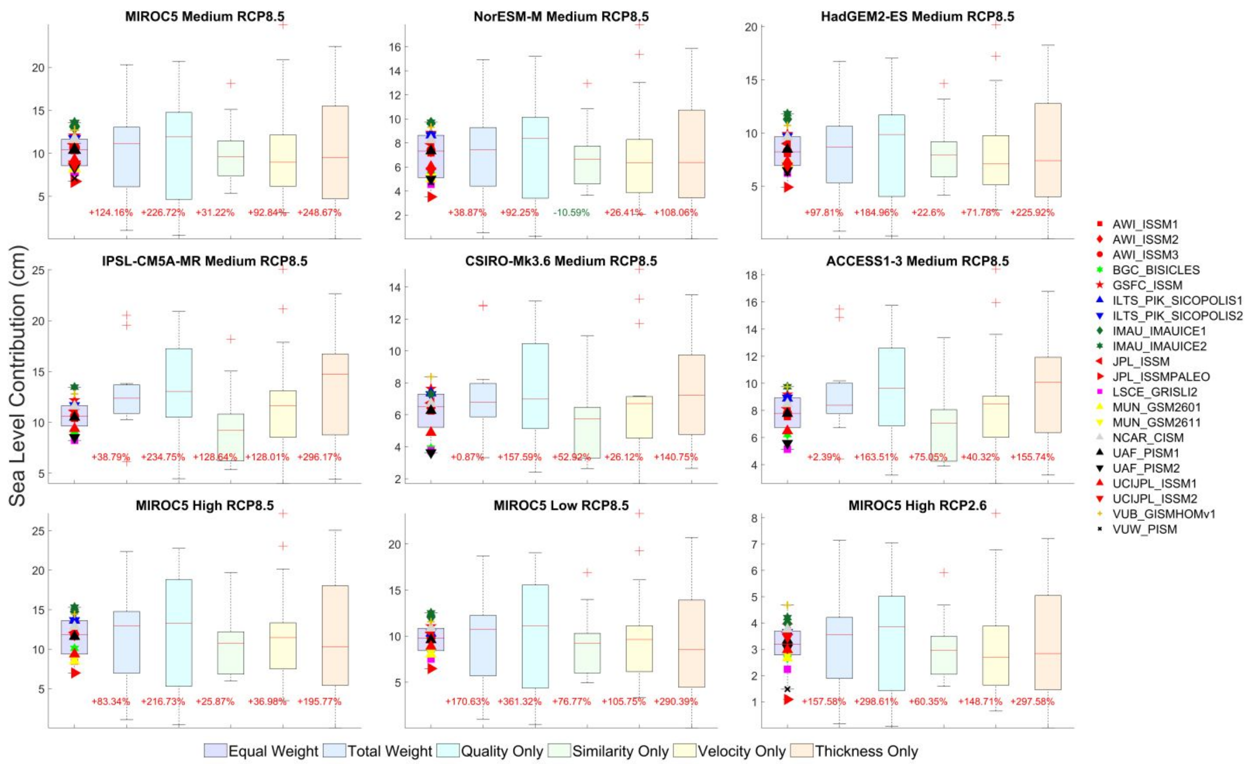

Fig. 8. Boxplots of the updated ISMIP6-Greenland projections in 2100 using varying weighting types including equal weights (original simulations), total weights, quality weights alone, similarity weights alone, velocity weights alone, and thickness weights alone. The original ISMIP6 projections are marked only on the first boxplot of each experiment. The text above each boxplot shows the reduction/increase of the model spread. The types of weighting scheme are indicated by the legends at the bottom.

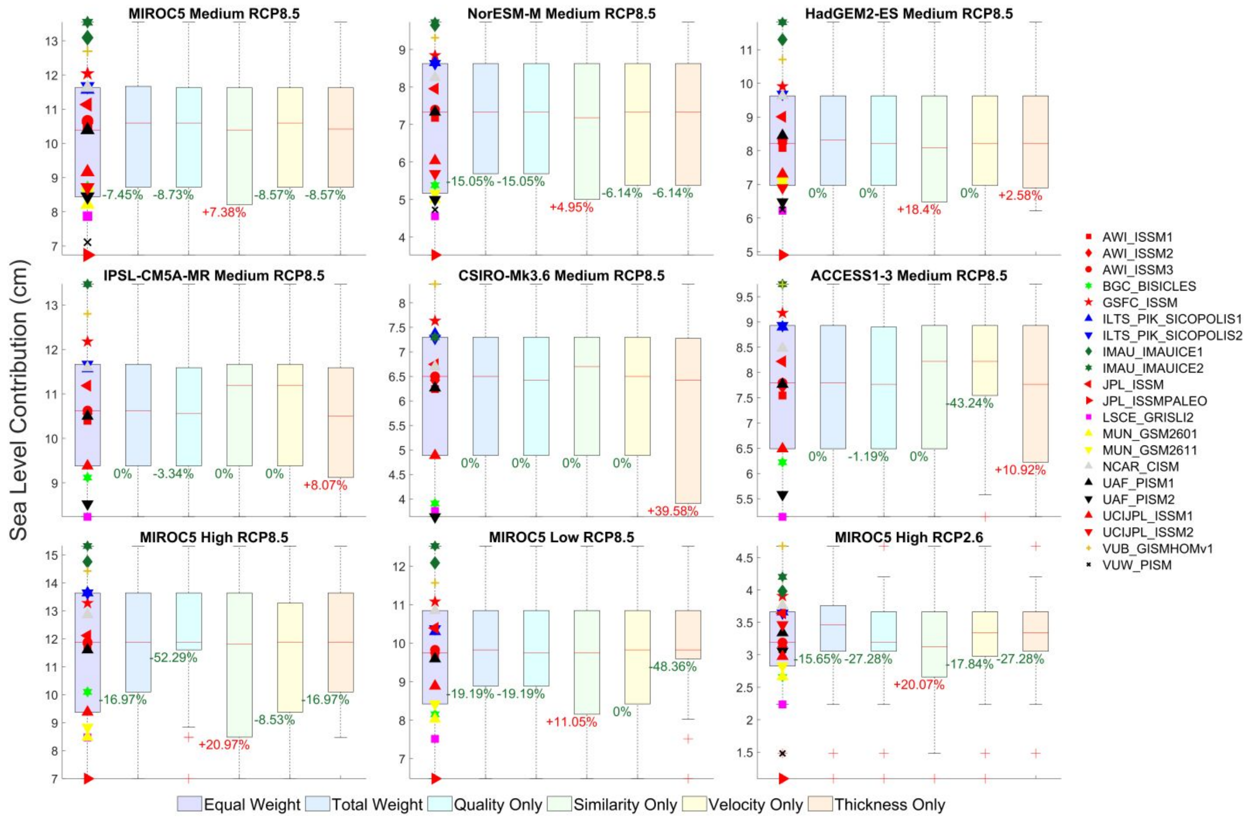

Fig. 9. Similar to Figure 8 but using Monte Carlo sampling approach as mentioned in the main text.

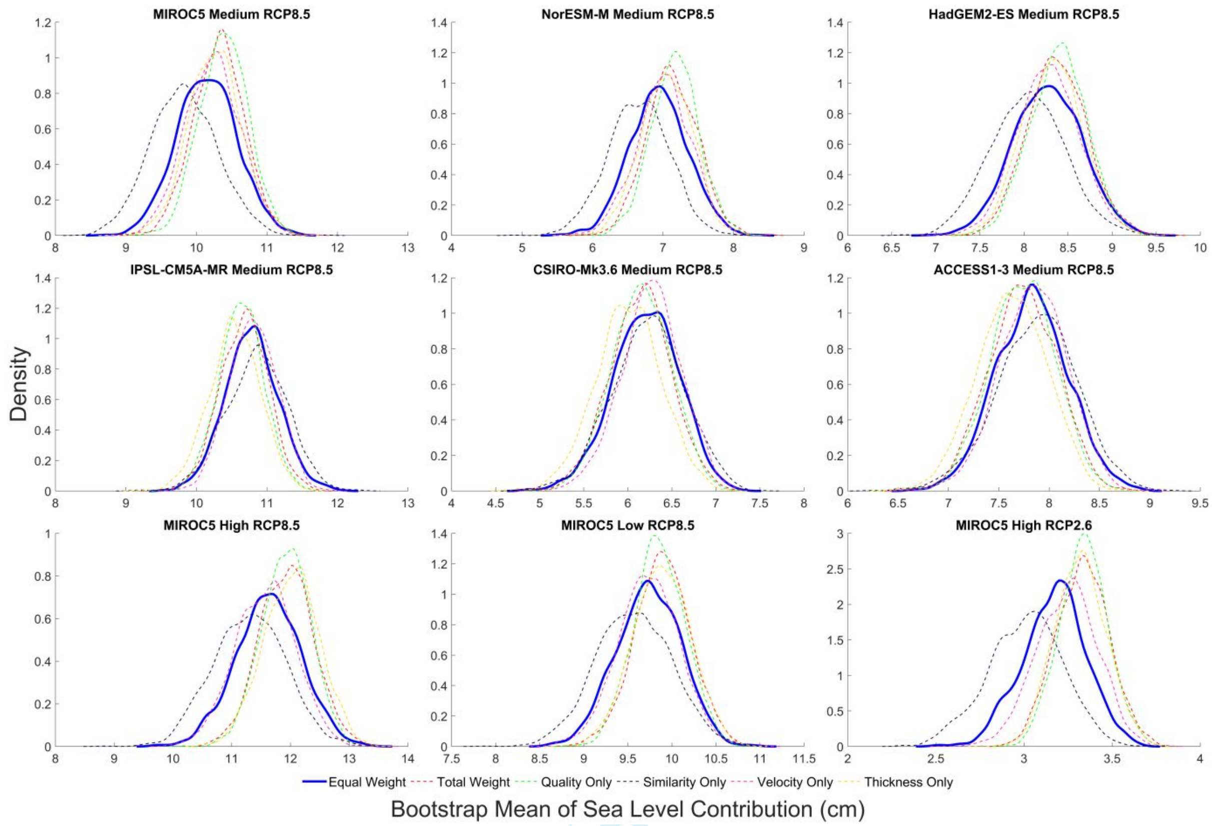

Fig. 10. Distributions of Bootstrap mean of ISMIP6-Greenland projections in 2100 using varying weighting types including equal weights (original simulations), total weights, quality weights alone, similarity weights alone, velocity weights alone, and thickness weights alone. The types of weighting scheme are indicated by the legends at the bottom.

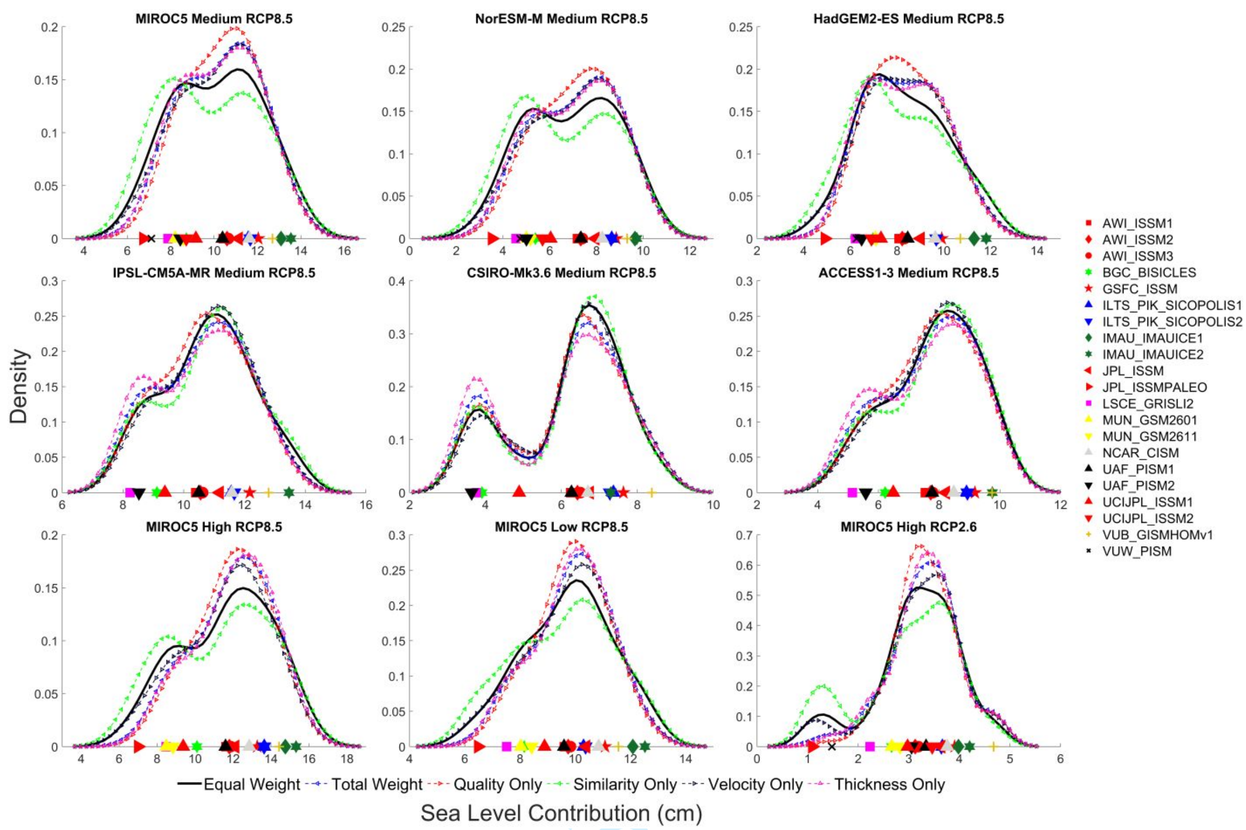

Fig. 11. Similar to Figure 10 but using KDE approach to estimate the distribution of sea level rise projections, in contrast to the estimation of ensemble mean shown in Figure 10. The individual ISMIP6 projections are marked on the x-axes as well.

4 Conclusions and discussion

In this study, we have used the ClimWIP model weighting strategy to assign weights to ISMIP6-Greenland ice sheet models to explore the influence on the sea level projections under model weights in contrast to "one model one vote" strategy, which is previously practiced in ISMIP6 literatures. This model weighting strategy considers both model performance compared to observation and model inter-dependence among the ensemble model participants. We choose ice velocity and thickness of the initial ice sheet state, which are the same diagnostics as in Goelzer and others (2020), to measure the model performance against observation. In contrast, we use as many ice sheet model variables as we can to assign the independence weights. Furthermore, we consider both the initial states and future projections to measure the independence weights. The motivation is that the models having similar initial states and multiple submissions (such as UAF_PISM) may respond very differently to climate forcing based on their implementation of ice-ocean interaction and other modeling options.

We also demonstrate the challenges of finding appropriate parameters involved in the model weighting scheme and how the choices of radius of quality (D_q) and similarity (D_u) can best facilitate the weighting. We select D_u as 0.5 times the mean of inter-model distance to effectively distinguish model differences, and we choose D_q as equal to the mean of inter-model distances so that the weighted ensemble shows decreased bias for both the present-day and future projections. For quality weighting, we found that the same model can have different performances when different diagnostics are used, which confirms the reasoning for using more than one single diagnostic. For example, UAF_PISM1 and PISM2 perform very differently when only one variable is used (Figures 7a and 7b), and the combined weights provide more balanced scores than the single variable scores. In the final model weighting results (Figure 7c), most models receive weights ranging from 0.3 to 0.5.

The model weights are then utilized to update the projections of the six Tier-1 experiments plus three Tier-2 experiments. We do not observe significant shifts of multi-model ensemble mean, but the model spreads are indeed reduced to varying extents depending on the experiments. The simple weighted standard deviations indicate around 10% to 30% of model spread reduction. We also explore four different ways to apply the model weights on the projections including the direct approach, Monte Carlo approach, Bootstrap mean approach, and Kernel Density Estimation approach to find the impacts on the distribution of projections. With the exception of the direct approach, which increases all model spreads, the other approaches generally reduce model spreads, but the magnitude of reduction varies significantly among experiments and types of model weights applied.

One limitation of this study is that we do not perform the tests regarding the choice of observation and correlation of diagnostics of ice sheet models with sea level rise projections and explore the influences of the types of diagnostics. As an exploratory study of assigning model weights on ISMIP6-Greeland models, we limit our focus merely on the same metrics used in Goelzer and others (2020). The Bayesian calibrations by using velocity change, dynamic ice thickness change, and mass change observations show very different posterior sea level rise distributions in Felikson and others (2023). Also, this study focuses on ISMIP6-Greenland model weighting, the same practice maybe used on ISMIP6-Antarctica (Seroussi and others, 2020) and ISMIP6-Antarctica-2300 in future research.

Another limitation arises from not exploring other model weighting schemes. For similarity weighting, the ClimWIP scheme stands on a data-driven point of view, that is, whether a pair of models are considered as similar models is judged by their initial states and simulation results. Other methods maybe used to sort the models, such as developing family model genealogy as recently practiced in the climate modeling community for CMIP6 models (Kuma and others, 2023).

We also note that the refinement of the updated sea level distribution is not as significant as the ones shown in the Bayesian calibration studies. However, they are not comparable due to the size of the ensemble. The size of the ensemble considered in Bayesian calibration tends to be much bigger (from several hundreds to thousands) in contrast to ISMIP6-Greenland models (21 models). This is because the ISMIP6-Greenland models generally submitted one realization (at most 3 realizations) for the same model. In contrast, the Bayesian calibration studies were designed to explore the uncertainties involved in the whole parameter space, resulting in a large number of perturbed ensemble members branching from the same model. This makes their prior distributions of probabilistic sea level rise (before Bayesian updating) very flat and the posterior much sharper.

In conclusion, we show in this study that the ClimWIP scheme is skillful in producing model weights that effectively and reasonably quantify the model performance and inter-dependency. The resulting projections show mild to medium level of decreased model spreads compared to the unweighted ensemble, although the multi-model mean does not have significant shift. This highlights the potential of applying model weights to reduce ensemble spreads for ice sheet intercomparison project, given that the next phase, i.e., ISMIP7, may include a bigger size of model submissions and experiments that can lead to larger ensemble uncertainties.

References

Aschwanden A, Fahnestock MA and Truffer M (2016) Complex Greenland outlet glacier flow captured. *Nature Communications* **7**(1), 10524. doi:10.1038/ncomms10524.

Aschwanden A and Brinkerhoff DJ (2022) Calibrated Mass Loss Predictions for the Greenland Ice Sheet. *Geophysical Research Letters* **49**(19), e2022GL099058. doi:10.1029/2022GL099058.

Bamber JL, Layberry RL and Gogineni SP (2001) A new ice thickness and bed data set for the Greenland ice sheet: 1. Measurement, data reduction, and errors. *Journal of Geophysical Research: Atmospheres* **106**(D24), 33773–33780. doi:10.1029/2001JD900054.

Bindschadler RA and others (2013) Ice-sheet model sensitivities to environmental forcing and their use in projecting future sea level (the SeaRISE project). *Journal of Glaciology* **59**(214), 195–224. doi:10.3189/2013JoG12J125.

Brinkerhoff D, Aschwanden A and Fahnestock M (2021) Constraining subglacial processes from surface velocity observations using surrogate-based Bayesian inference. *Journal of Glaciology* **67**(263), 385–403. doi:10.1017/jog.2020.112.

Brunner L, Pendergrass AG, Lehner F, Merrifield AL, Lorenz R and Knutti R (2020) Reduced global warming from CMIP6 projections when weighting models by performance and independence. *Earth System Dynamics* **11**(4), 995–1012. doi:10.5194/esd-11-995-2020.

Brunner L, Lorenz R, Zumwald M and Knutti R (2019) Quantifying uncertainty in European climate projections using combined performance-independence weighting. *Environmental Research Letters* **14**(12), 124010. doi:10.1088/1748-9326/ab492f.

DeConto RM and Pollard D (2016) Contribution of Antarctica to past and future sea-level rise. *Nature* **531**(7596), 591–597. doi:10.1038/nature17145.

Felikson D and others (2023) Choice of observation type affects Bayesian calibration of Greenland Ice Sheet model simulations. *The Cryosphere* **17**(11), 4661–4673. doi:10.5194/tc-17-4661-2023.

Fox-Kemper B and others (2021) 2021: Ocean, Cryosphere and Sea Level Change. In Climate Change 2021: The Physical Science Basis. Contribution of Working Group I to the Sixth Assessment Report of the Intergovernmental Panel on Climate Change. *Cambridge University Press, Cambridge, United Kingdom and New York, NY, USA*, 1211–1362. doi:10.1017/9781009157896.011.

Gladstone RM and others (2012) Calibrated prediction of Pine Island Glacier retreat during the 21st and 22nd centuries with a coupled flowline model. *Earth and Planetary Science Letters* **333–334**, 191–199. doi:10.1016/j.epsl.2012.04.022.

Goelzer H and others (2020) The future sea-level contribution of the Greenland ice sheet: a multi-model ensemble study of ISMIP6. *The Cryosphere* **14**(9), 3071–3096. doi:10.5194/tc-14-3071-2020.

Goelzer H and others (2018) Design and results of the ice sheet model initialisation experiments initMIP-Greenland: an ISMIP6 intercomparison. *The Cryosphere* **12**(4), 1433–1460. doi:10.5194/tc-12-1433-2018.

Hofer S and others (2020) Greater Greenland Ice Sheet contribution to global sea level rise in CMIP6. *Nature Communications* **11**(1), 6289. doi:10.1038/s41467-020-20011-8.

Jager E, Gillet-Chaulet F, Champollion N, Millan R, Goelzer H and Mouginot J (2024) The future of Upernavik Isstrøm through ISMIP6 framework: Sensitivity analysis and Bayesian calibration of ensemble prediction. *EGUsphere*, 1–45. doi:10.5194/egusphere-2024-862.

Joughin I, Smith H and Scambos T (2015) MEaSUREs Greenland Ice Sheet Velocity Map from InSAR Data, Version 2 [Data Set]. *Boulder, Colorado USA. NASA National Snow and Ice Data Center Distributed Active Archive Center*. https://doi.org/10.5067/OC7B04ZM9G6Q.

Knutti R, Sedláček J, Sanderson BM, Lorenz R, Fischer EM and Eyring V (2017) A climate model projection weighting scheme accounting for performance and interdependence. *Geophysical Research Letters* **44**(4), 1909–1918. doi:10.1002/2016GL072012.

Knutti R (2010) The end of model democracy? *Climatic Change* **102**(3), 395–404. doi:10.1007/s10584-010-9800-2.

Knutti R, Furrer R, Tebaldi C, Cermak J and Meehl GA (2010) Challenges in Combining Projections from Multiple Climate Models. *Journal of Climate* **23**(10), 2739–2758. doi:10.1175/2009JCLI3361.1.

Kuma P, Bender FA-M and Jönsson AR (2023) Climate Model Code Genealogy and Its Relation to Climate Feedbacks and Sensitivity. *Journal of Advances in Modeling Earth Systems* **15**(7), e2022MS003588. doi:10.1029/2022MS003588.

Larour E, Seroussi H, Morlighem M and Rignot E (2012) Continental scale, high order, high spatial resolution, ice sheet modeling using the Ice Sheet System Model (ISSM). *Journal of Geophysical Research: Earth Surface* **117**(F1). doi:10.1029/2011JF002140.

Lorenz R, Herger N, Sedláček J, Eyring V, Fischer EM and Knutti R (2018) Prospects and Caveats of Weighting Climate Models for Summer Maximum Temperature Projections Over North America. *Journal of Geophysical Research: Atmospheres* **123**(9), 4509–4526. doi:10.1029/2017JD027992.

Masson D and Knutti R (2011) Climate model genealogy. *Geophysical Research Letters* **38**(8). doi:10.1029/2011GL046864.

Merrifield AL, Brunner L, Lorenz R, Medhaug I and Knutti R (2020) An investigation of weighting schemes suitable for incorporating large ensembles into multi-model ensembles. *Earth System Dynamics* **11**(3), 807–834. doi:10.5194/esd-11-807-2020.

Morlighem M and others (2020) Deep glacial troughs and stabilizing ridges unveiled beneath the margins of the Antarctic ice sheet. *Nature Geoscience* **13**(2), 132–137. doi:10.1038/s41561-019-0510-8.

Morlighem M and others (2017) BedMachine v3: Complete Bed Topography and Ocean Bathymetry Mapping of Greenland From Multibeam Echo Sounding Combined With Mass Conservation. *Geophysical Research Letters* **44**(21), 11,051-11,061. doi:10.1002/2017GL074954.

Nias IJ, Nowicki S, Felikson D and Loomis B (2023) Modeling the Greenland Ice Sheet's Committed Contribution to Sea Level During the 21st Century. *Journal of Geophysical Research: Earth Surface* **128**(2), e2022JF006914. doi:10.1029/2022JF006914.

Nias IJ, Cornford SL, Edwards TL, Gourmelen N and Payne AJ (2019) Assessing Uncertainty in the Dynamical Ice Response to Ocean Warming in the Amundsen Sea Embayment, West Antarctica. *Geophysical Research Letters* **46**(20), 11253–11260. doi:10.1029/2019GL084941.

Nowicki S and others (2020) Experimental protocol for sea level projections from ISMIP6 stand-alone ice sheet models. *The Cryosphere* **14**(7), 2331–2368. doi:10.5194/tc-14-2331-2020.

Nowicki S and others (2013) Insights into spatial sensitivities of ice mass response to environmental change from the SeaRISE ice sheet modeling project II: Greenland. *Journal of Geophysical Research: Earth Surface* **118**(2), 1025–1044. doi:10.1002/jgrf.20076.

Payne AJ and others (2021) Future Sea Level Change Under Coupled Model Intercomparison Project Phase 5 and Phase 6 Scenarios From the Greenland and Antarctic Ice Sheets. *Geophysical Research Letters* **48**(16), e2020GL091741. doi:10.1029/2020GL091741.

Pennell C and Reichler T (2011) On the Effective Number of Climate Models. *Journal of Climate* **24**(9), 2358–2367. doi:10.1175/2010JCLI3814.1.

Rignot E and Mouginot J (2012) Ice flow in Greenland for the International Polar Year 2008–2009. *Geophysical Research Letters* **39**(11). doi:10.1029/2012GL051634.

Ritz C, Edwards TL, Durand G, Payne AJ, Peyaud V and Hindmarsh RCA (2015) Potential sea-level rise from Antarctic ice-sheet instability constrained by observations. *Nature* **528**(7580), 115–118. doi:10.1038/nature16147.

Sanderson BM, Wehner M and Knutti R (2017) Skill and independence weighting for multi-model assessments. *Geoscientific Model Development* **10**(6), 2379–2395. doi:https://doi.org/10.5194/gmd-10-2379-2017.

Sanderson BM, Knutti R and Caldwell P (2015) A Representative Democracy to Reduce Interdependency in a Multimodel Ensemble. *Journal of Climate* **28**(13), 5171–5194. doi:10.1175/JCLI-D-14-00362.1.

Seroussi H and others (2020) ISMIP6 Antarctica: a multi-model ensemble of the Antarctic ice sheet evolution over the 21st century. *The Cryosphere* **14**(9), 3033–3070. doi:10.5194/tc-14-3033-2020.

Shepherd A and others (2020) Mass balance of the Greenland Ice Sheet from 1992 to 2018. *Nature* **579**(7798), 233–239. doi:10.1038/s41586-019-1855-2.

Taylor KE (2001) Summarizing multiple aspects of model performance in a single diagram. *Journal of Geophysical Research: Atmospheres* **106**(D7), 7183–7192. doi:10.1029/2000JD900719.

Code and Data Availability

The ISMIP6 output data is accessible on https://theghub.org/. The BedMachine data is freely available on https://nsidc.org/data/nsidc-0756/versions/3. The MEaSUREs Greenland Ice Sheet Velocity Map from InSAR Data, Version 2 is freely available on https://nsidc.org/data/nsidc-0478/versions/2. The scripts used to generate the figures in this paper are available on XXX [zenodolink].

Acknowledgements

This research was supported by grants from the NASA Cryospheric Sciences, Sea Level Change Team and Modeling, Analysis and Predictions Program. We thank the Climate and Cryosphere (CliC) effort, which provided support for ISMIP6 through sponsoring of workshops, hosting the ISMIP6 website and wiki, and promoted ISMIP6. We acknowledge the World Climate Research Programme, which, through its Working Group on Coupled Modeling, coordinated and promoted CMIP5 and CMIP6. We thank the climate modeling groups for producing and making available their model output, the Earth System Grid Federation (ESGF) for archiving the CMIP data and providing access, the University at Buffalo for ISMIP6 data distribution and upload, and the multiple funding agencies who support CMIP5 and CMIP6 and ESGF. We thank the ISMIP6 steering committee, the ISMIP6 model selection group and ISMIP6 data set preparation group for their continuous engagement in defining ISMIP6.